Open access • Journal Article • DOI:10.1115/1.4023596

The Treatment of Nongray Properties in Radiative Heat Transfer: From Past to Present

Michael F. Modest

Published on: 01 Jun 2013 - Journal of Heat Transfer-transactions of The Asme (American Society of Mechanical Engineers)

The Treatment of Nongray Properties in Radiative Heat Transfer: From Past to Present

Michael F. Modest
Life Fellow ASME
University of California at Merced,
Merced, CA 95343
e-mail: MModest@ucmerced.edu

Radiative heat transfer in high-temperature participating media displays very strong spectral, or "nongray," behavior, which is both very difficult to characterize and to evaluate. This has led to very gradual development of nongray models, starting with primitive semigray and box models based on old experimental property data, to today's state-of-the-art k-distribution approaches with properties obtained from high-resolution spectroscopic databases. In this paper a brief review of the historical development of nongray models and property databases is given, culminating with a more detailed description of the most modern spectral tools. [DOI: 10.1115/1.4023596]

Keywords: radiative transfer, spectral models, band models, weighted-sum-of-gray-gases, k-distribution method

1 Introduction

The radiative transfer equation (RTE) that governs heat transfer by electromagnetic waves or photons is a five-dimensional partial differential equation (three in space, and two locally anchored direction coordinates), which is exceedingly difficult to solve. The problem is greatly exacerbated by the fact that radiative properties have spectral dependence, i.e., they vary across the spectrum as defined by wavelength λ, or wavenumber $\eta = 1/\lambda$. In the early years, when detailed information on the nongray behavior of participating media was not available and before the days of powerful computers, the aim of researchers commonly was to find an "equivalent" gray absorption coefficient to make calculations tractable. However, unlike in the case of surface transport, this generally leads to unacceptable errors, and was called by Edwards the "gray-gas myth" [1]. It is well-established today that treating gas absorption coefficients as gray in combustion systems may lead to temperature underpredictions of 100 °C or more [2]. Nevertheless, probably due to the great difficulties associated with spectral models, the practice persists to this day.

When the radiating medium is a gas, as found in combustion systems, chemical reactors, plasmas, etc., the radiative absorption coefficient is comprised of millions of narrow spectral lines caused by rotational, vibrational, and (at very high temperatures) electronic energy level transitions. Each spectral line is broadened slightly by several competing mechanisms, i.e., collision broadening (due to molecular collisions; dominant in most combustion systems and other applications at atmospheric or higher pressure), Doppler broadening (due to the Doppler effect from fast-moving molecules; dominant at high-altitude atmospheric sciences and astronautical applications), and Stark broadening (due to electric fields; important in charged plasmas). The result is an absorption coefficient that oscillates wildly across the spectrum, bunching up in so-called vibration–rotation bands (many rotational lines surrounding a single vibrational, and perhaps also electronic, transition). An example is given in Fig. 1, which shows the absorption coefficient for the 6.3 μm band of water vapor at 1000 K. Particulates, such as soot, coal particles, and aerosols, also have radiative properties that can display strong spectral dependencies. However, in most practical applications particles are either extremely small (soot), or have wide particle size distributions. In either case this leads to relatively benign (but strong) spectral variations (as compared to that of gases). However, larger particles may scatter radiation appreciably (necessitating cumbersome Lorenz–Mie calculations [3], and vastly complicating the RTE).

It is clear from Fig. 1 that accurate heat transfer calculations in the presence of radiating gases (and maybe accompanied by particulates) requires many (roughly 1×10^6) spectral evaluations of the RTE—if spectral knowledge of absorption coefficients is even available. Even with today's powerful computers and the advent of high-resolution spectroscopic databases are such line-by-line (LBL) solutions possible only for stand-alone benchmark problems. For practical applications the engineer must resort to approximate spectral models, and it is the purpose of this article to review how these "nongray" models have evolved over the past, say, 75 years.

2 Radiative Property Databases

The existence and structure of spectral lines has been known for quite some time from the development of quantum mechanics, as described; for example, in the classic books by Herzberg [4–6] and Penner [7]. Similarly, particle absorption and scattering properties have long been described with Maxwell's electromagnetic wave theory by Lorenz [8], Mie [9], and Debye [10], in what is known today as the Lorenz–Mie theory, and for very small particles already in the late 19th century by Lord Rayleigh [11]. Engineering level descriptions of the determination of spectral gas and particle properties may be found in standard textbooks, such as the ones by Modest [3] and Howell et al. [12], and exhaustive descriptions of particle properties have been given by van de Hulst [13] and Kerker [14]. The complicated spectral behavior of individual particles is of great importance in the atmospheric sciences [15], but in heat transfer applications their behavior tends to be benign [3,12] and will not be discussed here.

Experimental measurements of spectral radiative properties (and their incorporation into RTE solution methods) and/or the theoretical determination of spectral lines, have seen very gradual progress over the years. The earliest measurements of gas absorption coefficients apparently were total (i.e., nonspectral) data taken by Hottel, Mangelsdorf [16] and Eckert [17] in the 1930s, the former leading to the famous Hottel's charts [3,18,19]. Amazingly (shockingly?), these charts remain the only spectral information on combustion properties in virtually all undergraduate heat transfer texts to this very day. Hottel's total emissivity charts were

Manuscript received October 19, 2012; final manuscript received December 17, 2012; published online May 16, 2013. Assoc. Editor: Leslie Phinney.

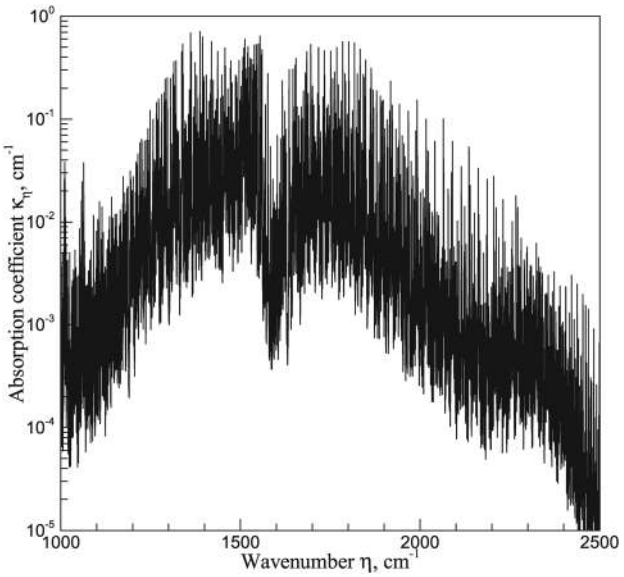

Fig. 1 Absorption coefficient of water vapor at 1000 K, 1 bar, and a mole fraction of 25% in nitrogen

later updated by Leckner [20], who also provided simple algebraic correlations. The first spectroscopic measurements were apparently conducted by Tingwaldt [21] (for carbon dioxide). Similar setups were described in the 1950s and 1960s by Howard et al. [22], Penner [7], Bevans et al. [23], and Tien and Giedt [24], leading to a plethora of narrowband data, i.e., data averaged over a small spectral range of 25–100 cm^{-1} (in fact, the present author's very first research paper used Tien's apparatus). For use in heat transfer calculations these data were correlated to obtain narrowband transmissivities, such as collected in the highly successful RADCAL database [25]; and they were employed to generate wideband (i.e., covering an entire vibration–rotation band) correlations [26]. Another narrowband database, assembled from high-resolution spectroscopic databases (discussed in the next paragraphs), has been made available by Soufiani and Taine [27] under the acronym EM2C. More detail on narrowband databases can be found by Modest [3].

During the past 40 years or so, due to the advent of high-resolution spectroscopy (mostly FTIR spectrometers), it has become possible to measure strengths and positions of individual spectral lines. A first collection of spectral data was assembled in the late 1960s by the Air Force Cambridge Research Laboratories for atmospheric scientists, including low-temperature data for the major constituents of the Earth's atmosphere, and was published in 1973 as an Air Force report [28]. With contributions from many researchers across the world this grew into the HITRAN database (an acronym for HIgh resolution TRANsmission molecular absorption), first published in 1987 [29]. The database is maintained by the Harvard–Smithsonian Center for Astrophysics, with periodic updates. The latest version at present is HITRAN 2008 [30], which includes detailed information on 39 species with a total of about 2.7×10^6 lines.

As the popularity of HITRAN grew, the need for a database valid at elevated temperatures became obvious. A first attempt was made by the group around Taine in France, who augmented HITRAN 1986 data for water vapor and carbon dioxide through theoretical calculations [31,32]. A development by the HITRAN group resulted in a first version of HITEMP (1995) [33] for H_2O, CO_2, CO, and OH, using theoretical models. Comparison with experiment [34,35] indicated that HITEMP 1995 greatly overpredicted CO_2 emissivities above 1000 K, while agreement for H_2O was acceptable. More accurate and extensive calculations for CO_2 were carried out in Russia, resulting in several versions of the CDSD-1000 database [36] (with the 2008 version containing 4×10^6 lines), which were shown to agree well with experiment. The latest version of CDSD, called CDSD-4000 [37], aims to be accurate up to 4000 K, and has 628×10^6 lines, requiring 23 GB of storage. Several extensive high-temperature collections were developed for H_2O: e.g., the Ames database [38] includes 300 million lines, and the BT2 collection [39] has 500 million lines. In 2010 a new version of HITEMP was released [40], designed for temperatures up to 3000 K. Citing best agreement against experimental data, HITEMP 2010 incorporates and extends CDSD 2008 for CO_2 (11×10^6 lines) and a slimmed-down version of BT2 for H_2O (111×10^6 lines). HITEMP 2010 also includes data for three diatomic gases (CN, CO, and OH) with their relatively few lines. An example calculation is given in Fig. 1, showing the 6.3 μm H_2O band, generated from the HITEMP 2010 database.

3 Total Emissivity Based Models

Historically, spectral models for the radiative transfer equation progressed along with the growing knowledge of spectral properties. Accordingly, early RTE models used total emissivity data to estimate heat transfer from combustion systems. The earliest and most successful of these models are the *mean beam length method* and the *weighted sum of gray gases method*, which were first advanced by Hottel [18] for the determination of radiative heat fluxes from an isothermal volume of hot combustion gases to cold black furnace walls. Detailed accounts of these methods have been given by Hottel [18] and Hottel and Sarofim [19], and more concise descriptions are included in modern textbooks [3,12].

3.1 Mean Beam Lengths. If we consider a hot nonscattering medium surrounded by cold black walls, the spectral flux onto a point on the surface is given by the impinging directional intensity I_η integrated over all 2π incoming solid angles, or [3]

$$q_\eta = \int_{2\pi} I_\eta \cos\theta d\Omega = \int_{2\pi}\int_{r=0}^{L(\hat{\mathbf{s}})} I_{b\eta} \exp\left(-\int_0^r \kappa_\eta dr'\right)\kappa_\eta \cos\theta dr d\Omega \tag{1}$$

where η is wavenumber, Ω is the solid angle, θ is the polar angle (incidence angle as measured from the surface normal), κ_η is the spectral absorption coefficient, $I_{b\eta}$ is the blackbody intensity (or Planck function), and $0 \le r \le L(\hat{\mathbf{s}})$ is the distance along a line to a point at the opposing surface (along a unit direction vector $\hat{\mathbf{s}}$). If the medium is homogeneous this may be simplified to

$$\begin{aligned} q_\eta &= I_{b\eta}\int_{2\pi}(1 - e^{-\kappa_\eta L(\hat{\mathbf{s}})})\cos\theta d\Omega = \pi I_{b\eta}(1 - e^{-\kappa_\eta L_e}) \\ &= \pi I_{b\eta}\epsilon_\eta(L_e) \end{aligned} \tag{2}$$

where—from the mean-value theorem—L_e is the *mean beam length* (radius of an equivalent hemisphere above the point where the heat flux is determined), and $\epsilon_\eta(L_e)$ is the spectral emissivity for a homogeneous gas column of length L_e. If the average flux onto an entire surface is desired the definition of the mean beam length L_e must be generalized accordingly. Note that the magnitude of the mean beam length depends on absorption coefficient as well as on geometry. However, Hottel noticed that the spectral heat flux q_η is not very sensitive to the spectral fluctuations of L_e, and that replacing the spectrally varying L_e by an *average mean beam length* L_m (independent of κ_η) predicts spectral heat fluxes with acceptable accuracy. For example, for the simple cases of homogeneous spheres and homogeneous, constant-thickness slabs the error never exceeds 5% if a suitable L_m is chosen. This statement may be generalized to other geometries. Values for the average mean beam lengths have been tabulated in several books, e.g., [3,12,19]. Employing an average value L_m allows the straightforward spectral integration of Eq. (2), resulting in a total heat flux of

$$q = \int_0^\infty q_\eta d\eta = \int_0^\infty \left(1 - e^{-\kappa_\eta L_m}\right) \pi I_{b\eta}(T) d\eta = \epsilon(L_m, T) \pi I_b(T)$$
$$= \epsilon(L_m, T) \sigma T^4 \tag{3}$$

where $\epsilon(L_m, T)$ is the total emissivity of an isothermal gas layer of thickness L_m.

3.2 Weighted Sum of Gray Gases. The concept of a weighted-sum-of-gray-gases (WSGG) approach was first presented by Hottel and Sarofim [19] within the framework of the zonal method. In this approach the nongray gas is replaced by a number of gray gases, which are related to the total emissivity of an isothermal column of length s by

$$\epsilon(T, s) \simeq \sum_{k=0}^{K} a_k(T)(1 - e^{-\kappa_k s}) \tag{4}$$

Hottel already made the physical argument that Eq. (4) implies a nongray absorption coefficient field comprising K different values κ_k arbitrarily distributed across the spectrum, and occupying a fraction $a_k(T)$ of the Planck function weighted spectrum. Values for the κ_k were found by curve-fitting total emissivity data and correlations, e.g., the ones by Truelove [41], Smith and coworkers [42], and others. The gray-gas absorption coefficients κ_k are constants, while the weight factors a_k may be functions of source temperature (wall temperature for the absorptivity and local medium temperature for emissivity). Neither a_k nor κ_k are allowed to depend on path length s. Since for an infinitely thick medium the emissivity and absorptivity approach unity, we find

$$\sum_{k=0}^{K} a_k(T) = 1 \tag{5}$$

However, for a pure molecular gas with its "spectral windows" between vibration–rotation bands it would take very large path lengths for the emissivity to be close to unity. For this reason Eq. (5) starts with $k = 0$ (with an implied $\kappa_0 = 0$), to allow for spectral windows. If the medium contains particles, such that $\kappa_\eta > 0$ always, the $k = 0$ term is simply dropped, i.e., $a_0 = 0$.

Modest [43] demonstrated in the early 1990s that this approach can be applied to the general radiative transfer equation and, therefore, to any RTE solution method (exact, P_N approximation, discrete ordinates method, etc.), provided all boundaries are black and the medium is nonscattering, resulting in K spectrally integrated RTEs

$$\frac{dI_k}{ds} = \kappa_k([a_k I_b] - I_k) \tag{6}$$

subject to the boundary condition

$$s = 0: \quad I_k = [a_k I_b](T_w) \tag{7}$$

for which the heat transfer rates are calculated independently. The total heat flux is then found by adding the heat fluxes of the gray gases, i.e.,

$$I(s) = \sum_{k=0}^{K} I_k(s), \quad \text{and} \quad \mathbf{q}(s) = \sum_{k=0}^{K} \mathbf{q}_k(s) \tag{8}$$

Depending on the material, the quality of the fit, and the accuracy desired, a K of 2 or 3 usually gives results of satisfactory accuracy [19]. Denison and Webb [44] showed a little later that the absorption coefficients κ_k do not need to be constant, and that the method is also valid for gray, reflecting walls. Indeed, if one applies the idea of a spectrally stepwise constant absorption coefficient directly to the RTE and integrates it over the K spectral regions, it is easily seen that the method holds in general, i.e., also for scattering media [45].

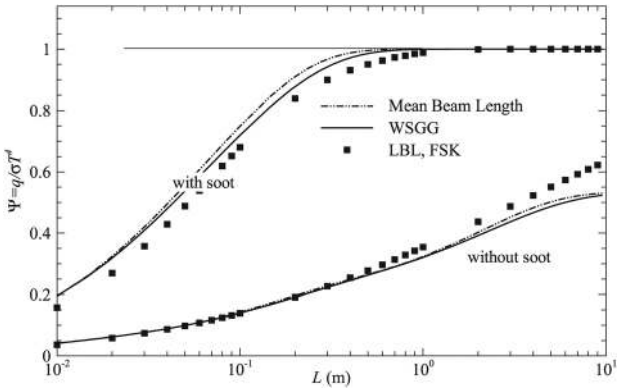

Fig. 2 Nondimensional heat loss from an isothermal N_2, H_2O, CO_2 mixture with and without soot [3]

An example is given in Fig. 2, which shows the heat loss from an isothermal slab at temperature $T = 1000$ K, and a total pressure of $p = 1$ atm. The slab consists of a mixture of 70% N_2, 20% H_2O, and 10% CO_2 (by volume), and is bordered by cold, black walls. The heat lost from the layer is also determined for the case that the gas is mixed with soot (density $\rho_p = 2000\,\mathrm{kg/m^3}$, volume fraction $f_v = 5 \times 10^{-6}$). Gray-gas coefficients are calculated from the correlation of Truelove [41], with 3 gray gases for the pure gas, and 2×3 gray gases for the soot–gas mixture. The heat loss from such a homogeneous layer, using the WSGG method, follows (in nondimensional form) as [3]

$$\Psi = \frac{q}{\sigma T^4} = \sum_{k=0}^{K} a_k[1 - 2E_3(\kappa_k L)] \tag{9}$$

where E_3 is an exponential integral function. The results are compared with "exact" LBL calculations, with spectral absorption coefficients obtained from the HITEMP 1995 database [33]. Without soot the WSGG method is seen to give results of very respectable accuracy, except for extremely long path lengths, for which the method underpredicts the gas emissivity somewhat. Differences are mostly due to the fact that the WSGG results employ old total emissivity data [18,19], and the LBL results are based on a modern spectroscopic database. Similar accuracy is obtained in the presence of soot (with some uncertainty about the nongray soot properties employed for the WSGG correlation).

For completeness, Fig. 2 also shows results from the simple mean beam length method, with total emissivities obtained from Eq. (4) with Truelove's WSGG coefficients [41], or

$$\Psi = \frac{q}{\sigma T^4} = \sum_{k=0}^{K} a_k[1 - e^{-\kappa_k L_m}], \quad L_m = 1.76L \tag{10}$$

It is observed that the mean beam length method also provides good accuracy for such simple problem (homogenous medium with cold black walls).

4 Band Based Models

If we limit ourselves to a nonscattering medium bounded by black walls, the spectral intensity along a single line of sight of length s is given by [3]

$$I_\eta(s) = I_{b\eta}(T_w) \exp\left[-\int_0^s \kappa_\eta ds'\right] + \int_0^s I_{b\eta}(T(s')) \exp\left[-\int_0^{s'} \kappa_\eta ds'\right] \kappa_\eta ds' \tag{11}$$

where T_w and $T(s')$ are wall and local gas temperature, respectively, with s' measured from s and toward the wall. The first term on the right-hand side is due to emission from the wall, attenuated by the transmissivity

$$t_\eta(s) = \exp\left[-\int_0^s \kappa_\eta ds'\right] \tag{12}$$

and the second term is emission from within the gas attenuated over a shorter path of length s'. It is clear from the spectral behavior of the absorption coefficient, as shown in Fig. 1, that the Planck function does not vary appreciably across a small spectral range of many lines, and we may define an average spectral transmissivity

$$\bar{t}_\eta(s) = \frac{1}{\Delta\eta}\int_{\eta-\Delta\eta/2}^{\eta+\Delta\eta/2} t_\eta(s)d\eta' = \frac{1}{\Delta\eta}\int_{\eta-\Delta\eta/2}^{\eta+\Delta\eta/2} \exp\left(-\int_0^s \kappa_\eta ds\right)d\eta' \tag{13}$$

Substituting the average spectral transmissivity into Eq. (11) gives an approximate expression for the average spectral intensity as

$$\bar{I}_\eta(s) = I_{b\eta}(T_w)\bar{t}_\eta(s) + \int_0^s I_{b\eta}(T(s'))\left|\frac{d\bar{t}_\eta}{ds'}\right|ds' \tag{14}$$

Equation (14) gives answers of excellent accuracy for narrowband averages of $\Delta\eta = 25\ \text{cm}^{-1}$ or less, and often still very respectable results if averages are taken over an entire vibration–rotation band (a "wideband").

4.1 Narrowband Models. To find spectrally averaged or "narrowband" values of the absorption coefficient and the transmissivity, some information must be available on the spacing of individual lines within the group and on their relative strengths. A number of models have been proposed for this purpose, of which the two extreme ones are the *Elsasser model*, in which equally spaced lines of equal intensity are considered, and the *statistical models*, in which the spectral lines are assumed to have random spacing and/or intensity. The Elsasser model, first proposed by Elsasser [46], is most appropriate for diatomic gases with a single vibrational energy mode. The first statistical models for more complicated molecules, with random line spacing and line intensity chosen from probability density functions (PDF), were proposed by Goody [47] and Godson [48,49], the latter with an improved PDF. All of these early models originated in the atmospheric sciences. A relative late comer is the Malkmus model [50], a product of NASA's space program, who recognized the importance of the abundance of extremely weak spectral lines and adjusted his line intensity PDF accordingly.

All narrowband models characterize line spacing and strengths through two nondimensional parameters, namely the *line overlap parameter* β, and the *narrowband optical thickness* τ, defined as

$$\beta = \pi\frac{\gamma}{d}, \quad \tau = \frac{S}{d}L \tag{15}$$

where γ is an average line *half-width at half height* (half its strength at line center), d is the average line spacing (both measured in cm^{-1}), S is the mean line strength (measured in cm^{-2}), and L is the length of the gas column. The spectral mean transmissivity for a homogeneous gas from the Malkmus model, the most successful of the statistical models, follows then as

$$\bar{t}_\eta(s) = \exp\left(-\frac{\beta}{2}\left[\sqrt{1+\frac{4\tau}{\beta}}-1\right]\right) \tag{16}$$

Inhomogeneous paths are difficult to treat within the narrowband models, and a number of approximate models have been proposed over the years. The most successful of these models is the Curtis–Godson two parameter scaling approximation [51]. In the Curtis–Godson approximation the values of τ and β used to calculate narrowband transmissivities (from the Elsasser or statistical models) are replaced by path-averaged values $\tilde{\tau}$ and $\tilde{\beta}$, determined from

$$\tilde{\tau} = \int_0^L \left(\frac{S}{d}\right)dx \tag{17}$$

$$\tilde{\beta} = \frac{1}{\tilde{\tau}}\int_0^L \frac{S}{d}\beta dx \tag{18}$$

The accuracy of various scaling approximations was tested by Hartmann and co-workers [52] for several nonhomogeneous conditions in CO_2–N_2 and H_2O–N_2 mixtures. It was found that the Malkmus model together with the Curtis–Godson scaling approximation generally gave the most accurate results.

The narrowband databases RADCAL [25] and EM2C [27] provide line overlap parameters β and narrowband optical thicknesses τ, as well as transmissivities calculated from the Malkmus model, for H_2O, CO_2 and CO. RADCAL also provides correlations for methane and soot, as well as transmissivities for nonhomogeneous paths using the Curtis–Godson model. Some results for one-dimensional slabs were obtained by Menart et al. [53] and by Cherkaoui and co-workers [54]. Multidimensional calculations were primarily carried out by the group around Liu, e.g., [55], for various combustion scenarios.

4.2 Wideband Models. While narrowband calculations are potentially the most accurate, provided an accurate database is used, they require a few hundred to a thousand spectral evaluations of the RTE. To limit the number of RTE solutions a number of wideband models, i.e., models predicting transmissivity (or emissivity) of an entire vibration–rotation band, were proposed. The simplest of them is the box model by Penner [7], with the band approximated by a rectangular box of width $\Delta\eta_e$ (the effective band width) and height $\overline{\kappa}$. By far the most successful of the wideband models is the exponential wideband model, first developed by Edwards and Menard [26], and further developed in a series of papers by Edwards and Balakrishnan [56]. The word "successful" here implies that the model is able to correlate experimental data for band absorptances

$$A = \int_{\text{band}} \epsilon_\eta d\eta = \int_{\text{band}} (1-t_\eta)d\eta \tag{19}$$

with an average error of approximately $\pm 20\%$ (but with maximum errors as high as 50% to 80%). In the exponential wideband model it is assumed that the mean spectral absorption coefficient $(S/d)_\eta$ decays exponentially away from the band center, as predicted by quantum mechanics [3]. Combining this with a statistical narrowband model (the Goody model, since the method was developed before the advent of the Malkmus model), this resulted in a model for the band absorptance in terms of three parameters correlated from experimental data, viz., a nominal band width ω (measured in cm^{-1}), a nondimensional band overlap parameter β (similar to its narrowband counterpart), and a band strength parameter, or integrated absorption coefficient

$$\alpha = \int_{\text{band}} \kappa_\eta d\eta = \int_{\text{band}} \left(\frac{S}{d}\right)_\eta d\eta \tag{20}$$

These parameters may be combined into nondimensional quantities to yield a two-parameter model for a nondimensional band absorptance,

$$A^* = \frac{A}{\omega} = f(\beta,\tau_0), \quad \tau_0 = \frac{\alpha}{\omega}L \tag{21}$$

where τ_0 is the optical thickness at the band center. Since Edwards' model consisted of several regime-dependent formulas, a number of single continuous correlations have also been proposed [57,58], the latter employing the superior Malkmus model. Wideband models face the same difficulties as narrowband models in the case of nonhomogeneous paths, and path-averaged values for $\tilde{\alpha}, \tilde{\beta}$, and $\tilde{\omega}$ must be found, as summarized by Edwards [1]. Numerous investigators have used the exponential wideband model for one-dimensional heat transfer calculations. We mention here only the more recent multidimensional calculations by Cumber and co-workers [59] (applying the RADCAL database to a jet flame with water vapor, CO_2, and soot), Liu et al. [60] (three-dimensional mixtures of water vapor, CO_2, and alumina particles, using the EM2C database), and Maruyama and Guo [61] (three-dimensional furnace with water vapor, CO_2, and carbon particles, using a spectral version of the wideband model combined with the Elsasser narrowband model).

4.3 *k*-Distributions. As noted earlier, over a small spectral interval, such as a few tens of wavenumbers, the Planck function (and other nongaseous radiation properties) remains essentially constant. Thus, across such a small spectral interval the intensity in a homogeneous medium varies with gas absorption coefficient alone. On the other hand, Fig. 1 shows that the gas absorption coefficient varies wildly even across a very narrow spectrum, attaining the same value for κ_η many times, each time producing the identical intensity field within the medium. Thus, carrying out line-by-line calculations across such a spectrum would be rather wasteful, repeating the same calculation again and again. It would, therefore, be advantageous to reorder the absorption coefficient field into a smooth, monotonically increasing function, assuring that each intensity field calculation is carried out only once. This was first recognized by the Armenian astrophysicist Viktor Hambardzumyan (or Ambartsumian) in Russia in the 1930s. The reordering idea was first reported in the Western literature by Arking and Grossman [62], giving credit to Kondratyev [63], who in turn credits a 1939 Ambartsumian paper. Other early publications on *k*-distributions are by Goody and co-workers [64], Lacis and Oinas [65], and Fu and Liou [66], all in the field of meteorology (atmospheric radiation). In the heat transfer area most of the early work on *k*-distributions is due to the group around Taine and Soufiani in France [27,67]. Unlike narrowband models, *k*-distributions are exact for homogeneous media and they can be applied directly to the RTE and its boundary conditions, i.e., the method is valid for scattering media and reflecting surfaces.

Historically, *k*-distributions $f(k)$ were first introduced using the spectrally averaged transmissivity $\bar{t}_\eta$:

$$\bar{t}_\eta(L) = \frac{1}{\Delta\eta}\int_{\Delta\eta} e^{-\kappa_\eta L} d\eta = \int_0^\infty e^{-kL} f(k) dk \tag{22}$$

The nature of *k*-distributions and how to evaluate them is best illustrated by looking at a very small part of the spectrum with very few lines. Figure 3(*a*) shows a fraction of the CO_2 15 μm band at 1 bar and 296 K and, to minimize irregularity, with only the strongest lines considered. It is seen that the absorption coefficient goes through a number of minima and maxima; between any two of these the integral may be rewritten as

$$\int e^{-\kappa_\eta L} d\eta = \int_{\kappa_{\eta,\min}}^{\kappa_{\eta,\max}} e^{-\kappa_\eta L} \left|\frac{d\eta}{d\kappa_\eta}\right| d\kappa_\eta$$

The absolute value sign comes from the fact that, where $d\kappa_\eta/d\eta < 0$, we have changed the direction of integration (always from $\kappa_{\eta,\min}$ to $\kappa_{\eta,\max}$). Therefore, integration over the entire range $\Delta\eta$ gives $f(k)$ as a weighted sum of the number of points where $\kappa_\eta = k$,

$$f(k) = \frac{1}{\Delta\eta}\sum_i \left|\frac{d\eta}{d\kappa_\eta}\right|_i = \frac{1}{\Delta\eta}\int_{\Delta\eta} \delta(k - \kappa_\eta) d\eta \tag{23}$$

where $\delta(k - \kappa_\eta)$ is the *Dirac-δ function*. The *k*-distribution of the absorption coefficient in Fig. 3(*a*) is shown as the thin solid line in Fig. 3(*b*), displaying very erratic behavior: Wherever the absorption coefficient has a maximum or minimum $f(k) \to \infty$ since $|d\kappa_\eta/d\eta| = 0$ at those points. Thankfully, the *k*-distribution itself is not needed during actual calculations. Introducing the *cumulative k-distribution* $g(k)$ as

$$g(k) = \int_0^k f(k) dk \tag{24}$$

we may rewrite the transmissivity (or any other narrowband averaged quantity) as

$$\bar{t}_\eta(L) = \int_0^\infty e^{-kL} f(k) dk = \int_0^1 e^{-k(g)L} dg \tag{25}$$

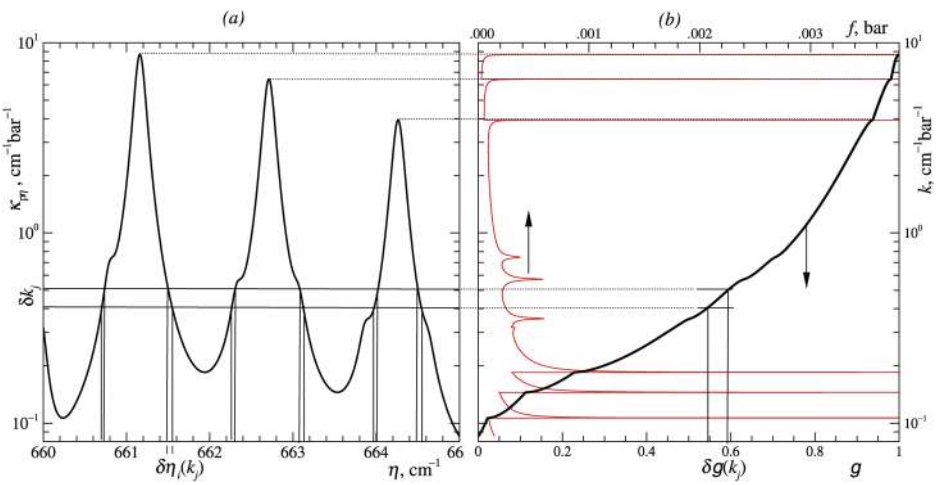

Fig. 3 Extraction of *k*-distributions from spectral absorption coefficient data: (*a*) simplified absorption coefficient across a small portion of the CO_2 15 μm band ($p = 1.0$ bar, $T = 296$ K); (*b*) corresponding *k*-distribution $f(k)$ and cumulative *k*-distribution $k(g)$ [3]

with $k(g)$ being the inverse function of $g(k)$, which is shown in Fig. 3(*b*) as the thick solid line. Sticking Eq. (24) into (23) leads to

$$g(k) = \int_0^k f(k)dk = \frac{1}{\Delta\eta}\int_{\Delta\eta}\int_0^k \delta(k-\kappa_\eta)dkd\eta = \frac{1}{\Delta\eta}\int_{\Delta\eta} H(k-\kappa_\eta)d\eta \tag{26}$$

where $H(k)$ is *Heaviside's unit step function*. Thus, $g(k)$ represents the fraction of the spectrum whose absorption coefficient lies below the value of k and, therefore, $0 \le g \le 1$. g acts as a nondimensional wavenumber (normalized by $\Delta\eta$), and the reordered absorption coefficient $k(g)$ is a smooth, monotonically increasing function, with minimum and maximum values identical to those of $\kappa_\eta(\eta)$.

In actual reordering schemes line-by-line values of k are grouped over small ranges $k_j \le k < k_j + \delta k_j = k_{j+1}$, as depicted in Fig. 3, so that

$$f(k_j)\delta k_j \simeq \frac{1}{\Delta\eta}\sum_i \left|\frac{\delta\eta}{\delta\kappa_\eta}\right|_i \delta k_j = \frac{1}{\Delta\eta}\sum_i \delta\eta_i(k_j) \tag{27}$$

where the summation over i collects all the occurrences where $k_j < \kappa_\eta < k_{j+1}$, and

$$g(k_{j+1}) = \sum_{j'=1}^{j} f(k_{j'})\delta k_{j'} = g(k_j) + f(k_j)\delta k_j \tag{28}$$

While generally a large number of k_j are chosen to assemble accurate k-distributions, Eq. (25) (and other narrowband quantities) are efficiently solved with few (6 to 16) quadrature points, using Gaussian or Gauss–Lobatto quadrature.

Like the statistical models the k-distributions are not straightforward to apply to nonhomogeneous paths. Two successful schemes for moderate inhomogeneities are the assumptions of *correlated* or *scaled* absorption coefficients.

Correlated k. It was found that for many important situations the k-distributions are essentially "correlated," i.e., if k-distributions $k(g)$ are known at two locations in a nonhomogeneous medium, then the absorption coefficient can essentially be mapped from one location to the other (documented to some extent by Lacis and Oinas [65]). This implies that all the values of η that correspond to one value of κ and g at one location, more or less map to the same value of g (but a different κ) at another location. We may then write, with good accuracy,

$$\bar{t}_\eta(L) = \frac{1}{\Delta\eta}\int_{\Delta\eta} \exp\left(-\int_0^L \kappa_\eta ds\right)d\eta \simeq \int_0^1 \exp\left(-\int_0^L k(s,g)ds\right)dg \tag{29}$$

This assumption of a correlated k-distribution has proven very successful in the atmospheric sciences, where temperatures change only from about 200 to 320 K, but pressure changes can be very substantial [64,65].

Scaled k. A more restrictive, but mathematically precise condition for correlation of k-distributions is to assume the dependence on wavenumber and location in the absorption coefficient to be separable, i.e.,

$$\kappa_\eta(\eta, T, P, x_a) = k_\eta(\eta)u(T, P, x_a) \tag{30}$$

where T and P are temperature and pressure of the gas, x_a is the mole fraction of the absorbing species, $k_\eta(\eta)$ is the absorption coefficient at some reference condition, and $u(T, p, p_a)$ is a nondimensional function depending on local conditions of the gas, but not on wavenumber. This is commonly known as the *scaling approximation*. Substituting this into Eq. (29) gives

$$\bar{t}_\eta(L) = \frac{1}{\Delta\eta}\int_{\Delta\eta} \exp\left(-k_\eta(\eta)\int_0^L u\,ds\right)d\eta = \frac{1}{\Delta\eta}\int_{\Delta\eta} \exp\left(-k_\eta\bar{u}L\right)d\eta \tag{31}$$

where $\bar{u}$ is now a path-integrated average for u. Comparing with Eq. (22), we find that in this case there is only a single k-distribution, based on the reference absorption coefficient k_η, and

$$\bar{t}_\eta(L) = \int_0^1 e^{-k(g)\bar{u}L}dg; \qquad \bar{u} = \frac{1}{L}\int_0^L uds \tag{32}$$

As for homogeneous media Eqs. (29) and (32) provide reordered absorption coefficients, which can be used in arbitrary radiation solvers without restrictions. At first glance, Eq. (29) looks superior to Eq. (32), since the assumption of a scaled absorption coefficient is more restrictive. However, in practice one needs to approximate an actual absorption coefficient, which is neither scaled nor correlated: If the scaling method is employed, the scaling function $u(T, p, p_a)$ and its reference state for k_η can be freely chosen and, thus, optimized for a problem at hand. On the other hand, if the correlated-k method is used, the absorption coefficient is simply *assumed* to be correlated (even though it is not), and the inherent error cannot be minimized.

Most narrowband k-distribution calculations to date have employed the EM2C k-distribution database [27], using the correlated-k assumption. A more accurate (and thus larger) narrowband k-distribution database has been reported by Wang and Modest [68]. Since databases are for single species, and since spectral information is lost in the reordering, mixing models needed to be generated to generate k-distributions from narrowband databases. The most successful is the uncorrelated-mixture model of Modest and Riazzi [69]. Marin and Buckius [70] applied the method to a one-dimensional slab containing water vapor or carbon dioxide (but not both) with fixed concentrations and varying temperatures (steps and parabolic profiles), noting that little loss of accuracy occurred for $\Delta\eta$ as large as 500 cm^{-1}. Dembele and co-workers used the method to determine radiation from fires with water spray curtains, using the discrete ordinates method and Mie scattering for the water droplets [71], and also to predict intensities exiting from a natural gas flame [72]. Tang and Brewster [73] also studied a one-dimensional slab containing CO_2, but included anisotropic scattering. Pierrot et al. [74,75] considered one-dimensional slabs containing H_2O and CO_2, as well, comparing various spectral solution methods. Liu et al. [76] tested different quadrature schemes for narrowband k-distribution calculations, and used the method for a three-dimensional geometry, to verify an approximate formulation of the statistical narrowband model applied to scattering media [76]. The method was further optimized and applied to several two-dimensional flames [77]. Finally, Tessé et al. [78] applied the method for the evaluation of turbulence–radiation interactions in turbulent flames.

5 Global Models

Global models are spectral models that deal with the entire spectrum at once. They include the very approximate total emissivity based models described in Sec. 3, as well as modern methods using high-resolution spectroscopic databases, which will be described in this section, viz., the *spectral line based weighted sum of gray gases* (SLW), the very similar *absorption distribution function* (ADF), and the *full spectrum k-distributions*.

5.1 Spectral Line Based Weighted Sum of Gray Gases (SLW). As indicated in Sec. 3 Hottel already made the physical argument that the weighted sum in Eq. (4) could also be

interpreted as a nongray absorption coefficient field comprising K different values κ_k arbitrarily distributed across the spectrum, and occupying a fraction $a_k(T)$ of the Planck function weighted spectrum. Using this argument Denison and Webb [79,80] collected distribution functions for absorption cross sections as

$$F_s(C_{\text{abs}}, T_b, T_g, P, x_s) = \frac{\pi}{\sigma T_b^4} \sum_i \int_{\Delta\eta \in (C_{\text{abs},\eta}(T_g,P,x_s) < C_{\text{abs}})} I_{b\eta}(T_b) d\eta \tag{33}$$

where the sum is over all spectral regions $\Delta\eta$ for which $C_{\text{abs},\eta}(T_g, P, x_s) < C_{\text{abs}}$. Here T_g is gas temperature, P is total pressure, x_s is mole fraction of species s, and the molar absorption cross section is related to the absorption coefficient by

$$C_{\text{abs},\eta} = \frac{R_u T_g}{P x_s} \kappa_\eta \tag{34}$$

with R_u being the universal gas constant. In a numerical calculation, the absorption cross-section domain is divided into discrete increments and a solution is found for each increment represented by a single value of the absorption cross section or a single gray gas. For example, for a homogeneous gas with a single absorbing species, in the absence of scattering and within a black-walled enclosure one obtains

$$\frac{dI_i}{ds} = \tilde{k}_i(T)(\bar{a}_i(T) I_b(T) - I_i), \quad i = 1, \ldots, K \tag{35}$$

for the K gray gases, subject to the boundary condition

$$I_{wi} = \bar{a}_i(T_w) I_b(T_w) \tag{36}$$

The weight function $\bar{a}_i$ in Eq. (35) is

$$\bar{a}_i(T) = F_s(C_{\text{abs},i}, T, T, P, x_s) - F_s(C_{\text{abs},i-1}, T, T, P, x_s) \tag{37}$$

while for the boundary condition $\bar{a}_i$ is evaluated as

$$\bar{a}_i(T_w) = F_s(C_{\text{abs},i}, T_w, T, P, x_s) - F_s(C_{\text{abs},i-1}, T_w, T, P, x_s) \tag{38}$$

Thus, $\bar{a}_i$ is the ith finite range of the distribution function evaluated at the *local* Planck function temperature (T or T_w). The $\tilde{k}_i$ is an average value over the range $F_{i-1} < F_s \le F_i$. Denison and Webb [79,80] suggest to evaluate k_i from a square-root average, i.e.,

$$\tilde{k}_i(T) = \sqrt{k(T, F_{i-1}) k(T, F_i)} \tag{39}$$

with k related to C_{abs} through Eq. (34). Inspection of Eqs. (6) and (7) shows that the SLW scheme is simply the weighted-sum-of-gray-gases method, with absorption coefficients k_i and weights a_i evaluated from a line-by-line database. An example for a homogeneous CO_2–N_2 mixture is given in Fig. 4, with corresponding heat transfer results in Fig. 5. Results are given for SLW parameters calculated directly from the HITEMP 2010 database, and for parameters found from a simple correlation [81]; also included are LBL results, and values obtained with the full-spectrum k-distribution method of the following section. In this example $K = 5$ was chosen, which—as seen from Fig. 5—results in respectable accuracy over a considerable range of optical thickness.

Denison and Webb also applied the SLW method to nonhomogeneous media, for which they deduced that the weight function $\bar{a}_i$ should be evaluated from

$$\bar{a}_i(T, \underline{\phi}_0) = F_s(C_{\text{abs},i}, T, \underline{\phi}_0) - F_s(C_{\text{abs},i-1}, T, \underline{\phi}_0) \tag{40}$$

where $\underline{\phi} = (T, P, x_s)$ is a vector defining the local gas state, and $\underline{\phi}_0 = (\overline{T}_0, P_0, x_{s,0})$ is a reference state. Thus, $\bar{a}_i$ is the ith finite range of the distribution function evaluated at the *local* Planck function temperature, while κ is evaluated at the reference state. The $\tilde{k}_i$ is calculated as

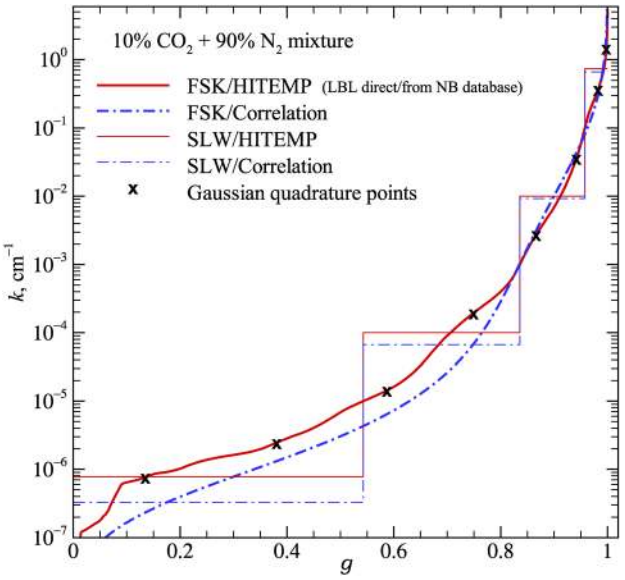

Fig. 4 Planck function weighted cumulative *k*-distributions for 10% CO_2 in nitrogen for gas and Planck function temperatures of 1000 K, as evaluated from the HITEMP database and the correlation by Modest [3]

$$\tilde{k}_i(T_0, \underline{\phi}) = \sqrt{k_{i-1}(T_0, \underline{\phi}) k_i(T_0, \underline{\phi})} \tag{41}$$

i.e., the value from the distribution function evaluated with the *local* absorption coefficient and the Planck function evaluated at the *reference* temperature. These rather complicated relationships for $\bar{a}$ and k_i were correctly deduced by Denison and Webb [80], well before a solid theoretical foundation describing the interrelationships between k-distributions was developed by Modest [82].

Rivière and co-workers employed the SLW method, but evaluated the gray gas parameters differently, calling it the absorption distribution function (ADF) model [74]. The same group

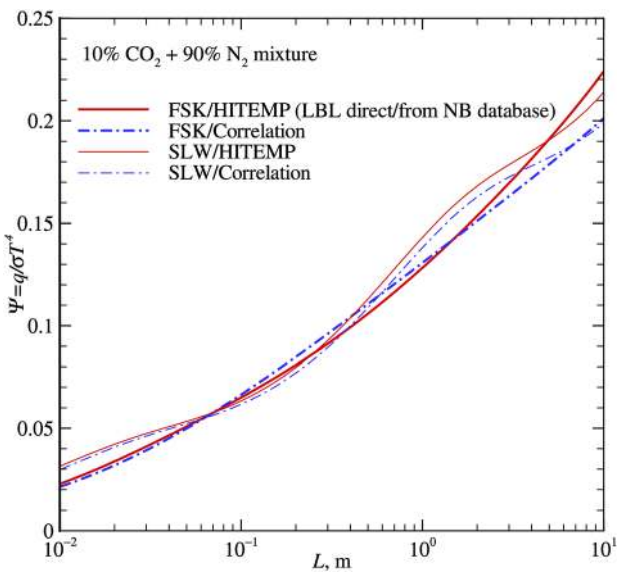

Fig. 5 Heat loss from an isothermal slab of 10% CO_2 in nitrogen at $T = 1000$ K, as evaluated from the LBL, FSK, and SLW models [3]

recognized that for the case of strong temperature inhomogeneities one may separate a gas into a number of "fictitious gases," grouping spectral lines according to the values of their lower level energies, calling it the absorption distribution function fictitious gases method [75].

5.2 Full Spectrum *k*-Distributions (FSK). In the full spectrum k-distribution (FSK) method, like its narrowband counterpart of Sec. 4.3, the absorption coefficient is reordered into a monotonically increasing function. However, in the full spectrum case allowance must be made for a blackbody intensity (or Planck function) varying across the spectrum. The FSK method can be developed very much like a narrowband k-distribution via a gas column transmissivity (or absorptivity), clearly showing its close relationship with the WSGG approach. This has been described in the original paper by Modest and Zhang [45]. The FSK method can also be applied directly to the RTE, resulting in a more powerful derivation, because it shows that the approach is also valid for arbitrarily scattering media and for arbitrarily reflecting surfaces, as long as the absorption coefficient remains the only spectrally varying radiative property [45,82]. In this section we will first consider the simple case of a homogeneous medium, i.e., a medium with uniform temperature, pressure, and mixture mole fraction throughout. Such a mixture has an absorption coefficient that, while varying across the spectrum, is spatially constant. The radiative transfer equation for such a medium is [3]

$$\frac{dI_\eta}{ds} = \kappa_\eta I_{b\eta} - (\kappa_\eta + \sigma_s) I_\eta + \frac{\sigma_s}{4\pi}\int_{4\pi} I_\eta(\hat{\mathbf{s}}')\Phi(\hat{\mathbf{s}},\hat{\mathbf{s}}')d\Omega' \tag{42}$$

where—in order to establish a global model—scattering coefficient σ_s and phase function Φ are assumed to be independent of wavenumber (gray). Let Eq. (42) be subject to the boundary conditions at a wall

$$I_\eta = I_{w\eta} = \epsilon_w I_{bw\eta} + (1-\epsilon_w)\frac{1}{\pi}\int_{\hat{\mathbf{n}}\cdot\hat{\mathbf{s}}<0} I_\eta |\hat{\mathbf{n}}\cdot\hat{\mathbf{s}}| d\Omega \tag{43}$$

where $I_{w\eta}$ is the spectral intensity leaving the enclosure wall, due to (diffuse gray) emission with emittance ϵ_w and/or (diffuse gray) reflection, and $\hat{\mathbf{n}}$ is a unit surface normal pointing into the medium.

A full spectrum k-distribution is defined, in accordance with Eq. (23) for a narrowband, as

$$f(T,k) = \frac{1}{I_b}\int_0^\infty I_{b\eta}(T)\delta(k-\kappa_\eta)d\eta \tag{44}$$

The $f(T,k)$ in Eq. (44) is a *Planck-function-weighted k-distribution* and is a function of temperature through the blackbody intensity. A reordered RTE is obtained by multiplying Eqs. (42) and (43) by the Dirac-δ function $\delta(k-\kappa_\eta)$, followed by integration over the entire spectrum and, finally, division by the k-distribution. This leads to

$$\frac{dI_g}{ds} = k\big(I_b(T) - I_g\big) - \sigma_s\left(I_g - \frac{1}{4\pi}\int_{4\pi} I_g(\hat{s}')\Phi(\hat{s},\hat{s}')d\Omega'\right) \tag{45}$$

with boundary condition

$$I_g = I_{wg} = \epsilon_w a(T_w,T,g) I_{bw} + (1-\epsilon_w)\frac{1}{\pi}\int_{\hat{\mathbf{n}}\cdot\hat{\mathbf{s}}<0} I_g|\hat{\mathbf{n}}\cdot\hat{\mathbf{s}}|d\Omega \tag{46}$$

where

$$I_g = \int_0^\infty I_\eta \delta\big(k-\kappa_\eta\big)d\eta / f(T,k) \tag{47}$$

$$g(T,k) = \int_0^k f(T,k)dk = \frac{1}{I_b}\int_0^\infty I_{b\eta}(T)H(k-\kappa_\eta)d\eta \tag{48}$$

$$a(T_w,T,g) = \frac{f(T_w,k)}{f(T,k)} = \frac{dg_w(T_w,k)}{dg(T,k)} \tag{49}$$

Physically, the cumulative k-distribution g is the Planck-function-weighted fraction of the spectrum with absorption coefficient $\kappa_\eta < k$ and, as inspection of Eq. (33) shows, is identical to Denison and Webb's distribution function. The total intensity is evaluated from

$$I = \int_0^\infty I_\eta d\eta = \int_0^\infty I_g f(T,k)dk = \int_0^1 I_g dg \tag{50}$$

In Eq. (49) the numerator and denominator are both evaluated at identical values of k, which in turn are related to g through Eq. (48). Note that two Planck-function weighted k-distributions are required: one at the temperature of the homogeneous medium $f(T,k)$, and one evaluated at the wall temperature $f(T_w,k)$, but both using the absorption coefficient evaluated at the conditions of the medium. Unfortunately, full spectrum k-distributions vary significantly with their method of evaluation, span across many orders of magnitude, and may be quite ill-behaved, much like their narrowband counterparts (cf. Fig. 3). However, as noted in Sec. 4.3, the sharp peaks in $f(T,k)$ are due to maxima and minima of κ_η, which remain the same for all Planck function temperatures. Consequently, the ratio of any two full spectrum k-distributions evaluated at different Planck function temperatures produces a much smoother function.

Cumulative k-distributions (or absorption distribution functions) are cumbersome to assemble and, for that reason, several narrowband k-distribution databases have been reported, from which full-spectrum k-distributions can be constructed [27,68]. A number of simple (and rather approximate) analytical full-spectrum k-distribution correlations have also been developed [79,81,83–85]. For gas mixtures mixing can be done more accurately on a narrowband level, but more cheaply at the full spectrum level. Again, the Modest and Riazzi [69] has been shown to be the most accurate, with the Solovjov and Webb [86] multiplicative mixing model for the full spectrum being somewhat less accurate but computationally cheaper.

It is important to understand that the FSK method given by Eqs. (45) through (49) is an *exact* method (subject to the restrictions of a homogeneous medium). In fact, the method is also exact for nonhomogeneous media, provided the absorption coefficient is spatially invariant (e.g., evaluated at a reference condition and then applied to the entire medium), or is *correlated* (as defined earlier). Within these restrictions the FSK results are equivalent to LBL calculations, the former requiring roughly 10 spectral evaluations versus about 1,000,000 for LBL. A sample result is shown in Fig. 5. The thick solid line in Fig. 5 shows results from direct LBL calculations and from the FSK method with k-distributions assembled from the Wang and Modest database [68], i.e., they are indistinguishable. The thick dash-dot line shows FSK results obtained with the analytical correlation of Modest and Mehta [81], which offers good accuracy except for large L (when small k become important, which are not emphasized in the correlation).

Comparison with the SLW method (or the WSGG method with its parameters based on a spectral line database) shows that, mathematically, the SLW scheme is in effect a crude implementation of the FSK method, using a simple step function integration over the spectrum.

Like for all other spectral models, extension of the FSK method to inhomogeneous media is not trivial. For moderately inhomogeneous media one can with good success assume the absorption coefficient to be *correlated* or *scaled*, as described in Sec. 4.3, with the correlated approach being a bit simpler and more popular. Again, a

reordered RTE is obtained by multiplying Eqs. (42) and (43) by the Dirac-δ function $\delta(k-\kappa_\eta(\underline{\phi}_0))$, with κ_η evaluated at a carefully chosen reference state $\underline{\phi}_0$, followed by integration over the entire spectrum and division by the reference state k-distribution. This leads to

$$\frac{dI_g}{ds} = k(T_0,\underline{\phi},g)\left[a(T,T_0,g)I_b(T) - I_g\right] - \sigma_s\left(I_g - \frac{1}{4\pi}\int_{4\pi} I_g(\hat{s}')\Phi(\hat{s},\hat{s}')d\Omega'\right) \tag{51}$$

provided that the absorption coefficient is correlated, i.e., at every wavenumber across the entire spectrum, where $\kappa_\eta(\eta,\underline{\phi}_0)=k$, we must also have a unique value for $\kappa_\eta(\eta,\underline{\phi})=k^*(\underline{\phi},k)$ (which may be a function of k, but not of η). Here

$$I_g = \int_0^\infty I_\eta \delta\left(k-\kappa_\eta(\eta,\underline{\phi}_0)\right)d\eta/f(T_0,\underline{\phi}_0,k) \tag{52}$$

$$g(T_0,\underline{\phi}_0,k) = \int_0^k f(T_0,\underline{\phi}_0,k)dk \tag{53}$$

$$a(T,T_0,g) = \frac{f(T,\underline{\phi}_0,k)}{f(T_0,\underline{\phi}_0,k)} = \frac{dg(T,\underline{\phi}_0,k)}{dg(T_0,\underline{\phi}_0,k)} \tag{54}$$

In Eq. (54) the numerator and denominator are both evaluated at identical values of k, but with k-distributions evaluated at different Planck function temperatures. Like for Eq. (49), the stretching parameter a is best evaluated by taking the ratio of the gradients of (slightly smoothened) cumulative k-distributions g. Three different k-distributions are required: $k(T_0,\underline{\phi},g)$ is the k-distribution evaluated with the absorption coefficient at *local* conditions and the Planck function at the *reference* temperature, while for the stretching factor $a(T,T_0,g)$ k-distributions are needed with the absorption coefficient at *reference* conditions, and the Planck function evaluated at both local and reference temperatures.

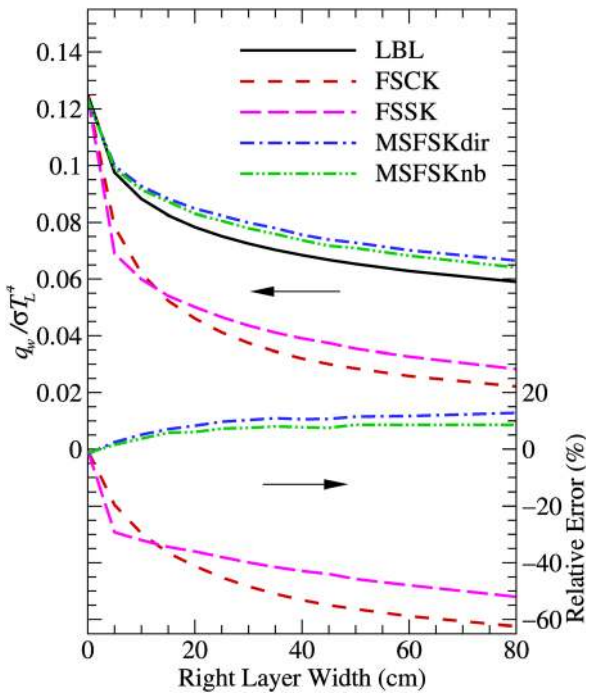

Fig. 6 Relative errors of the FSCK, FSSK, MSFSKdir, and MSFSKnb calculations for heat fluxes leaving from the right side of a two-layer slab with step changes in temperature and mole fraction. Left layer (50 cm width): 1500 K, 2% CO_2 and 20% H_2O; right layer (varying width): 500 K, 20% CO_2 and 2% H_2O [87].

An example is given in Fig. 6 for a very inhomogeneous case, with steps in temperature and mole fractions of the two radiating species CO_2 and H_2O. For such artificially extreme cases the FSK becomes rather inaccurate (whether one uses the here-discussed *correlated FSK*, FSCK, or the *scaled FSK*, FSSK). In the limit of a zero-width right layer one has a homogeneous medium and all FSK methods are exact. As the thickness of the cold right layer increases, the absorption coefficient becomes more and more uncorrelated, with errors exceeding 60% in the prediction of the radiative flux exiting from the cold layer. To accommodate strong gradients in temperature and concentrations (including particles) several higher-order models have also been developed, viz., the multiscale FSK (MSFSK: the gas mixture is broken up into "scales," placing *spectral lines* into separate scales according to their behavior) [75,87,88], the multigroup FSK (MGFSK: the gas mixture is broken up into "groups," placing *wavenumbers* into separate groups according to the temperature dependence of the spectral absorption coefficients) [89], and a hybrid multigroup, multiscale FSK (MGMSFSK) [90]. In the multiscale approach lines from a single gas species may be separated according to their temperature dependence (also known as "fictitious gases") [75,87] to improve accuracy in a gas with strong temperature gradients. More effectively, entire species are placed into scales to accommodate uncorrelatedness from locally varying concentrations. For example, for a methane–air flame one may collect CO_2 and H_2O into one scale (since they, approximately, occur together everywhere with a 1:2 ratio), and methane into a second (since methane exists where there is little CO_2 and H_2O, and *vice versa*). In the hybrid scheme species are first separated into scales (according to their concentration levels), and then the spectrum of each scale is broken into wavenumber groups (according to their temperature behavior). Figure 6 also includes results from a two-scale MSFSK model, with CO_2 and H_2O each being a scale (with k-distributions calculated directly from the spectroscopic databases, or from a narrowband k-distribution database [68]). As can be seen, the MSFSK approach alleviates the uncorrelatedness due to the concentration step, reducing the maximum error to about 10%. In physically meaningful applications with more benign gradients the basic FSK method can be expected to be much more accurate and may suffice in most cases.

As a final, realistic, and two-dimensional example we consider an axisymmetric ethylene–air jet flame experimentally studied by Kent and Honnery [91]. The burner of this flame has a cylindrical nozzle of diameter $d_j = 3$ mm, with Reynolds number varying from 7500 to 15,000. Details of the numerical simulation may be found in Mehta et al. [92]. The converged results of that study were used as a frozen data field for radiation calculations. CO_2, H_2O, CO, and soot are the major products of combustion and hence are considered in radiation calculations in addition to ethylene (fuel). Details of the flow field and the radiation calculations are given by Pal and Modest [90]; we show here in Fig. 7 only the local radiative heat source term calculated using the LBL approach, and the errors incurred by the basic FSK, the MSFSK, and the 2 and 4 group MSMGFSK approaches, with all k-distributions assembled from narrowband databases, and employing the P-1 method as the RTE solver. Relative errors are determined by comparison with LBL as

$$\text{error}(\%) = \frac{\nabla\cdot\mathbf{q}_{\text{LBL}} - \nabla\cdot\mathbf{q}_{\text{FSK/MSFSK/MSMGFSK}}}{\nabla\cdot\mathbf{q}_{\text{LBL,max}}}\times 100 \tag{55}$$

Figure 7(*b*) shows that the basic FSK method is accurate to about 3% across most of the flame, occupied by gas–soot mixtures with varying ratios of concentrations (in particular in regions of large $\nabla\cdot\mathbf{q}$). However, near the nozzle (with large amounts of C_2H_4 and few combustion products) the gas becomes very uncorrelated and the maximum error in the present problem reaches as much as

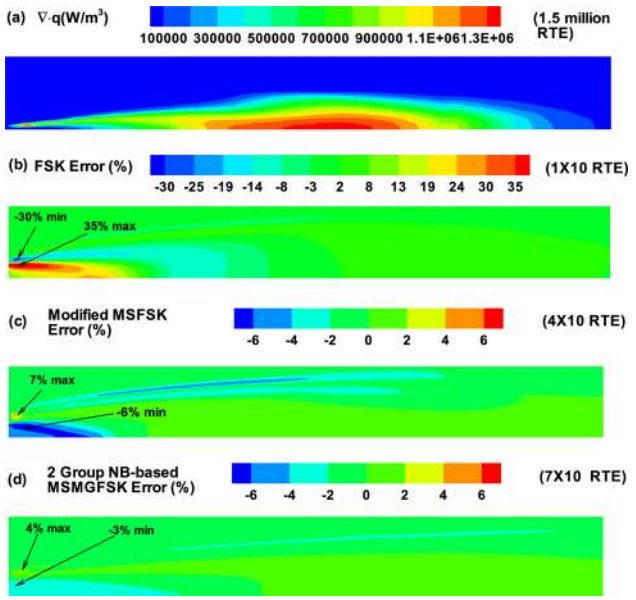

Fig. 7 (*a*) Local radiative heat source using LBL method and relative error (compared to LBL) for heat source calculations using (*b*) the single-scale FSK method; (*c*) the MSFSK method; and (*d*) the 2 group MSMGFSK method [90]

35% near the inlet. In the multiscale approach, CO_2 and H_2O are combined into a single scale since they have approximately the same ratio of concentration throughout the combustion chamber, while C_2H_4, CO, and soot are treated as single-group individual scales. The maximum error is now limited to 7% near the inlet (region of high errors) as seen in Fig. 7(*c*). Figure 7(*d*) shows the errors incurred in the 2 group narrowband based MSMGFSK calculations. In this approach the C_2H_4, CO, and soot are treated as single-group scales while CO_2 and H_2O are treated as two separate scales each having two spectral groups. The maximum error for this case is limited to 4%. The results from the 4 group-based MSMGFSK method are approximately the same as the 2 group case and are not shown here. CPU time required for the LBL calculations is approximately 56 h on a 2.4 GHz AMD Opteron machine while the basic FSK, the MSFSK, the 2 group-based MSMGFSK, and the 4 group-based MSMGFSK take only 7, 41, 78, and 110 s (i.e., typical times required for chemistry calculations in a combustion problem), respectively. This implies factors of 3×10^4, 5×10^3, 2.5×10^3, and 2×10^3 CPU time improvement, respectively, over LBL cost.

While the SLW and FSK methods are still research tools (i.e., most publications are developments by the original developers) these sophisticated spectral models are also being used by other researchers in various applications. For example, Mazumder and Modest [93] tested the correlated FSK scheme for a 2D environment, Sun and Smith [94] incorporated it into a backward Monte Carlo scheme, and Porter et al. [95] applied the FSK method to oxy-fuel combustion. The latter tested the method against much more expensive statistical narrowband calculations and found the FSK to be equally accurate. Demarco et al. [96] recently compared various spectral models for nonsooting media, including narrowband models, SLW and FSK, and concluded that the FSK method provided the best accuracy at a reasonable computational cost. Narrowband *k*-distributions were first applied in the field of atmospheric sciences; the full-spectrum versions developed by the heat transfer community have since then found their way back to the atmospheric sciences [97,98]. The concept may be applied to any system with strong spectrally varying radiation, and has most recently also been used to determine nonequilibrium radiation in hypersonic plasmas [99,100].

6 Summary

The past 75 years have seen tremendous advances in the heat transfer area, and none more significant than in the field of thermal radiation, where models and measurements have progressed from contrived one-dimensional, gray problems to high-fidelity diagnoses and simulations of full-scale combustion systems with their complicated spectral radiation behavior. In this article we have given a review of the progress in the determination of spectral radiation properties of combustion gases, ranging from early total spectrum measurements in the 1930s, to the narrowband measurements of the 1950s through 1980s, and culminating with high-resolution FTIR experiments and theoretical predictions leading to today's spectroscopic databases listing many millions of spectral lines. We reviewed how spectral models progressed in the same time frame, starting with total emissivity correlations in the 1950s, followed by narrowband and wideband models in support of narrowband measurements, and culminating with a description of the modern *k*-distributions, from early narrowband *k*-distributions to today's state-of-the-art global models, the spectral line based weighted sum of gray gases (SLW) and full spectrum *k*-distribution (FSK) models and their derivatives. It was concluded that high-fidelity global models have progressed to the point that they achieve near-LBL accuracy at a tiny fraction of the computational cost, making it possible today to include high-accuracy thermal radiation models in simulations of complicated combustion systems.

References

[1] Edwards, D. K., 1976, "Molecular Gas Band Radiation," *Advances in Heat Transfer*, Vol. 12, Academic, New York, pp. 115–193.
[2] Wang, L., Modest, M. F., Haworth, D. C., and Turns, S. R., 2005, "Modeling Nongray Soot and Gas-Phase Radiation in Luminous Turbulent Nonpremixed Jet Flames," Combust. Theory Model., **9**(3), pp. 479–498.
[3] Modest, M. F., 2013, *Radiative Heat Transfer*, 3rd ed., Academic, New York.
[4] Herzberg, G., 1944, *Atomic Spectra and Atomic Structure*, 2nd ed., Van Nostrand, New York.
[5] Herzberg, G., 1945, *Molecular Spectra and Molecular Structure, Vol. II: Infrared and Raman Spectra of Polyatomic Molecules*, Van Nostrand, Princeton, NJ.
[6] Herzberg, G., 1950, *Molecular Spectra and Molecular Structure, Vol. I: Spectra of Diatomic Molecules*, 2nd ed., Van Nostrand, Princeton, NJ.
[7] Penner, S. S., 1960, *Quantitative Molecular Spectroscopy and Gas Emissivities*, Addison-Wesley, Reading, MA.
[8] Lorenz, L., 1890, *Videnskab Selskab Skrifter*, Vol. 6, Kongelige Danske Videnskabernes Selskab, Copenhagen, Denmark.
[9] Mie, G., 1908, "Beiträge zur Optik Trüber Medien, Speziell Kolloidaler Metallösungen," Ann. Phys., **330**, pp. 377–445.
[10] Debye, P., 1909, "Der Lichtdruck auf Kugeln von Beliebigem Material," Ann. Phys., **335**(11), pp. 57–136.
[11] Rayleigh, Lord, 1871, "On the Light From the Sky, Its Polarization and Colour," Philos. Mag., **41**, pp. 107–120, 274–279 (Reprinted in Scientific Papers by Lord Rayleigh, Vol. I: 1869–1881, No. 8, Dover, New York, 1964).
[12] Howell, J. R., Siegel, R., and Mengüç, M. P., 2002, *Thermal Radiation Heat Transfer*, 4th ed., Taylor and Francis, New York.
[13] van de Hulst, H. C., 1957, *Light Scattering by Small Particles*, John Wiley, New York.
[14] Kerker, M., 1969, *The Scattering of Light and Other Electromagnetic Radiation*, Academic, New York.
[15] Goody, R. M., and Yung, Y. L., 1989, *Atmospheric Radiation: Theoretical Basis*, 2nd ed., Oxford University Press, New York.
[16] Hottel, H. C., and Mangelsdorf, H. G., 1935, "Heat Transmission by Radiation From Non-Luminous Gases II. Experimental Study of Carbon Dioxide and Water Vapor," Trans. AIChE, **31**, pp. 517–549.
[17] Eckert, E. R. G., 1937, "Messung der Gesamtstrahlung von Wasserdampf und Kohlensäure in Mischung mit Nichtstrahlenden Gasen bei Temperaturen bis 1300 °C," VDI Forschungshefte, **387**, pp. 1–20.
[18] Hottel, H. C., 1954, "Radiant Heat Transmission," *Heat Transmission*, 3rd ed., W. H. McAdams, ed., McGraw-Hill, New York, Chap. 4.
[19] Hottel, H. C., and Sarofim, A. F., 1967, *Radiative Transfer*, McGraw-Hill, New York.
[20] Leckner, B., 1972, "Spectral and Total Emissivity of Water Vapor and Carbon Dioxide," Combust. Flame, **19**, pp. 33–48.
[21] Tingwaldt, C., 1938, "The Absorbtion of Carbonic Acid in the Range of Lambda=4.3 mu Between 300 Degrees and 1000 Degrees Absolute," Phys. Z., **39**, pp. 1–6 (in German).
[22] Howard, D. N., Burch, D. E., and Williams, D., 1956, "Infrared Transmission of Synthetic Atmospheres—1: Instrumentation," J. Opt. Soc. Am., **46**(3), pp. 186–190.
[23] Bevans, J. T., Dunkle, R. V., Edwards, D. K., Gier, J. T., Levenson, L. L., and Oppenheim, A. K., 1960, "Apparatus for the Determination of the Band

Absorption of Gases at Elevated Pressures and Temperatures," J. Opt. Soc. Am., **50**, pp. 130–136.
[24] Tien, C. L., and Giedt, W. H., 1965, "Experimental Determination of Infrared Absorption of High-Temperature Gases," *Advances in Thermophysical Properties at Extreme Temperatures and Pressures*, ASME, New York, pp. 167–173.
[25] Grosshandler, W. L., 1993, "RADCAL: A Narrow-Band Model for Radiation Calculations in a Combustion Environment," NIST Technical Note 1402, National Institute of Standards and Technology.
[26] Edwards, D. K., and Menard, W. A., 1964, "Comparison of Models for Correlation of Total Band Absorption," Appl. Opt., **3**, pp. 621–625.
[27] Soufiani, A., and Taine, J., 1997, "High Temperature Gas Radiative Property Parameters of Statistical Narrow-Band Model for H_2O, CO_2, and CO, and Correlated-k Model for H_2O and CO_2," Int. J. Heat Mass Transfer, **40**(4), pp. 987–991.
[28] McClatchey, R. A., Benedict, W. S., Clough, S. A., Burch, D. E., Fox, K., Rothman, L. S., and Garing, J. S., 1973, "AFCRL Atmospheric Absorption Line Parameters Compilation," Technical Report No. AFCRL-TR-0096.
[29] Rothman, L. S., Gamache, R. R., Goldman, A., Brown, L. R., Toth, R. A., Pickett, H. M., Poynter, R. L., Flaud, J.-M., Camy-Peyret, C., Barbe, A., Husson, N., Rinsland, C. P., and Smith, M. A. H., 1987, "The HITRAN Database: 1986 Edition," Appl. Opt., **26**(19), pp. 4058–4097.
[30] Rothman, L. S., Gordon, I. E., Barbe, A., Benner, D. C., Bernath, P. F., Birk, M., Boudon, V., Brown, L. R., Campargue, A., Champion, J.-P., Chance, K., Coudert, L. H., Dana, V., Devi, V. M., Fally, S., Flaud, J.-M., Gamache, R. R., Goldman, A., Jacquemart, D., Kleiner, I., Lacome, N., Lafferty, W. J., Mandin, J.-Y., Massie, S. T., Mikhailenko, S. N., Miller, C. E., Moazzen-Ahmadi, N., Naumenko, O. V., Nikitin, A. V., Orphal, J., Perevalov, V. I., Perrin, A., Predoi-Cross, A., Rinsland, C. P., Rotger, M., Simeckova, M., Smith, M. A. H., Sung, K., Tashkun, S. A., Tennyson, J., Toth, R. A., Vandaele, A. C., and Auwera, J. V., 2009, "The HITRAN 2008 Molecular Spectroscopic Database," J. Quant. Spectrosc. Radiat. Transfer, **110**, pp. 533–572.
[31] Scutaru, D., Rosenmann, L., and Taine, J., 1994, "Approximate Band Intensities of CO_2 Hot Bands at 2.7, 4.3 and 12 μm for High Temperature and Medium Resolution Applications," J. Quant. Spectrosc. Radiat. Transfer, **52**, pp. 765–781.
[32] Rivière, P., Langlois, S., Soufiani, A., and Taine, J., 1995, "An Approximate Data Base of H_2O Infrared Lines for High Temperature Applications at Low Resolution. Statistical Narrow-Band Model Parameters," J. Quant. Spectrosc. Radiat. Transfer, **53**, pp. 221–234.
[33] Rothman, L. S., Wattson, R. B., Gamache, R. R., Schroeder, J., and McCann, A., 1995, "HITRAN HAWKS and HITEMP: High-Temperature Molecular Database," Proc. SPIE, **2471**, pp. 105–111.
[34] Fleckl, T., Jäger, H., and Obernberger, I., 2002, "Experimental Verification of Gas Spectra Calculated for High Temperatures Using the HITRAN/HITEMP Database," J. Phys. D: Appl. Phys., **35**(23), pp. 3138–3144.
[35] Bharadwaj, S. P., and Modest, M. F., 2007, "Medium Resolution Transmission Measurements of CO_2 at High Temperature—An Update," J. Quant. Spectrosc. Radiat. Transfer, **103**, pp. 146–155.
[36] Tashkun, S. A., and Perevalov, V. I., 2008, "Carbon Dioxide Spectroscopic Databank (CDSD): Updated and Enlarged Version for Atmospheric Applications," 10th HITRAN Conference, Cambridge, MA, Paper T2.3. Available at ftp://ftp.iao.ru/pub/CDSD-2008
[37] Tashkun, S. A., and Perevalov, V. I., 2011, "CDSD-4000: High-Resolution, High-Temperature Carbon Dioxide Spectroscopic Databank," J. Quant. Spectrosc. Radiat. Transfer, **112**(9), pp. 1403–1410.
[38] Partridge, H., and Schwenke, D. W., 1997, "The Determination of an Accurate Isotope Dependent Potential Energy Surface for Water From Extensive Ab Initio Calculations and Experimental Data," J. Chem. Phys., **106**(11), pp. 4618–4639.
[39] Barber, R. J., Tennyson, J., Harris, G. J., and Tolchenov, R. N., 2006, "A High-Accuracy Computed Water Line List," Mon. Not. R. Astron. Soc., **368**, pp. 1087–1094.
[40] Rothman, L. S., Gordon, I. E., Barber, R. J., Dothe, H., Gamache, R. R., Goldman, A., Perevalov, V. I., Tashkun, S. A., and Tennyson, J., 2010, "HITEMP, the High-Temperature Molecular Spectroscopic Database," J. Quant. Spectrosc. Radiat. Transfer, **111**(15), pp. 2139–2150.
[41] Truelove, J. S., 1975, "The Zone Method for Radiative Heat Transfer Calculations in Cylindrical Geometries," HTFS Design Report DR33 (Part I: AERE-R8167), Atomic Energy Authority, Harwell, UK.
[42] Smith, T. F., Shen, Z. F., and Friedman, J. N., 1982, "Evaluation of Coefficients for the Weighted Sum of Gray Gases Model," ASME J. Heat Transfer, **104**(4), pp. 602–608.
[43] Modest, M. F., 1991, "The Weighted-Sum-of-Gray-Gases Model for Arbitrary Solution Methods in Radiative Transfer," ASME J. Heat Transfer, **113**(3), pp. 650–656.
[44] Denison, M. K., and Webb, B. W., 1993, "A Spectral Line-Based Weighted-Sum-of-Gray-Gases Model for Arbitrary RTE Solvers," ASME J. Heat Transfer, **115**(4), pp. 1004–1012.
[45] Modest, M. F., and Zhang, H., 2002, "The Full-Spectrum Correlated-k Distribution for Thermal Radiation From Molecular Gas–Particulate Mixtures," ASME J. Heat Transfer, **124**(1), pp. 30–38.
[46] Elsasser, W. M., 1943, *Heat Transfer by Infrared Radiation in the Atmosphere*, Harvard University Press, Cambridge, MA.
[47] Goody, R. M., 1952, "A Statistical Model for Water-Vapour Absorption," Q. J. R. Meteorol. Soc., **78**, pp. 165–169.
[48] Godson, W. L., 1955, "The Computation of Infrared Transmission by Atmospheric Water Vapour," J. Meteor., **12**, pp. 272–284.
[49] Godson, W. L., 1955, "The Computation of Infrared Transmission by Atmospheric Water Vapour, Part II," J. Meteor., **12**, pp. 533–535.
[50] Malkmus, W., 1967, "Random Lorentz Band Model With Exponential-Tailed S^{-1} Line-Intensity Distribution Function," J. Opt. Soc. Am., **57**(3), pp. 323–329.
[51] Young, S. J., 1977, "Nonisothermal Band Model Theory," J. Quant. Spectrosc. Radiat. Transfer, **18**, pp. 1–28.
[52] Soufiani, A., Hartmann, J.-M., and Taine, J., 1985, "Validity of Band-Model Calculations for CO_2 and H_2O Applied to Radiative Properties and Conductive–Radiative Transfer," J. Quant. Spectrosc. Radiat. Transfer, **33**, pp. 243–257.
[53] Menart, J. A., Lee, H. S., and Kim, T. K., 1993, "Discrete Ordinates Solutions of Nongray Radiative Transfer With Diffusely Reflecting Walls," ASME J. Heat Transfer, **115**(1), pp. 184–193.
[54] Cherkaoui, M., Dufresne, J.-L., Fournier, R. Grandpeix, J.-Y., and Lahellec, A., 1998, "Radiative Net Exchange Formulation Within One-Dimensional Gas Enclosures With Reflective Surfaces," ASME J. Heat Transfer, **120**(1), pp. 275–278.
[55] Liu, F., 1999, "Numerical Solutions of Three-Dimensional Non-Grey Gas Radiative Transfer Using the Statistical Narrow-Band Model," ASME J. Heat Transfer, **121**(1), pp. 200–203.
[56] Edwards, D. K., and Balakrishnan, A., 1973, "Thermal Radiation by Combustion Gases," Int. J. Heat Mass Transfer, **16**, pp. 25–40.
[57] Felske, J. D., and Tien, C. L., 1974, "A Theoretical Closed Form Expression for the Total Band Absorptance of Infrared-Radiating Gases," ASME J. Heat Transfer, **96**, pp. 155–158.
[58] Wang, W. C., 1983, "An Analytical Expression for the Total Band Absorptance of Infrared-Radiating Gases," J. Quant. Spectrosc. Radiat. Transfer, **29**, pp. 279–281.
[59] Cumber, P. S., Fairweather, M., and Ledin, H. S., 1998, "Application of Wide Band Radiation Models to Non-Homogeneous Combustion Systems," Int. J. Heat Mass Transfer, **41**(11), pp. 1573–1584.
[60] Liu, F., Smallwood, G. J., and Gülder, Ö. L., 1999, "Application of Statistical Narrowband Model to Three-Dimensional Absorbing–Emitting–Scattering Media," J. Thermophys. Heat Transfer, **13**(3), pp. 285–291.
[61] Maruyama, S., and Guo, Z., 1999, "Radiative Heat Transfer in Arbitrary Configurations With Nongray Absorbing, Emitting, and Anisotropic Scattering Media," ASME J. Heat Transfer, **121**(3), pp. 722–726.
[62] Arking, A., and Grossman, K., 1972, "The Influence of Line Shape and Band Structure on Temperatures in Planetary Atmospheres," J. Atmos. Sci., **29**, pp. 937–949.
[63] Kondratyev, K. Y., 1969, *Radiation in the Atmosphere*, Academic, New York.
[64] Goody, R. M., West, R., Chen, L., and Crisp, D., 1989, "The Correlated k Method for Radiation Calculations in Nonhomogeneous Atmospheres," J. Quant. Spectrosc. Radiat. Transfer, **42**, pp. 539–550.
[65] Lacis, A. A., and Oinas, V., 1991, "A Description of the Correlated-k Distribution Method for Modeling Nongray Gaseous Absorption, Thermal Emission, and Multiple Scattering in Vertically Inhomogeneous Atmospheres," J. Geophys. Res., **96**(D5), pp. 9027–9063.
[66] Fu, Q., and Liou, K. N., 1992, "On the Correlated k-Distribution Method for Radiative Transfer in Nonhomogeneous Atmospheres," J. Atmos. Sci., **49**(22), pp. 2139–2156.
[67] Rivière, P., Scutaru, D., Soufiani, A., and Taine, J., 1994, "A New c–k Data Base Suitable From 300 to 2500 K for Spectrally Correlated Radiative Transfer in CO_2–H_2O Transparent Gas Mixtures," 10th International Heat Transfer Conference, Taylor & Francis, London, pp. 129–134.
[68] Wang, A., and Modest, M. F., 2005, "High-Accuracy, Compact Database of Narrow-Band k-Distributions for Water Vapor and Carbon Dioxide," J. Quant. Spectrosc. Radiat. Transfer, **93**, pp. 245–261.
[69] Modest, M. F., and Riazzi, R. J., 2005, "Assembly of Full-Spectrum k-Distributions From a Narrow-Band Database; Effects of Mixing Gases, Gases and Nongray Absorbing Particles, and Mixtures With Nongray Scatterers in Nongray Enclosures," J. Quant. Spectrosc. Radiat. Transfer, **90**(2), pp. 169–189.
[70] Marin, O., and Buckius, R. O., 1997, "Wide Band Correlated-k Approach to Thermal Radiative Transport in Nonhomogeneous Media," ASME J. Heat Transfer, **119**(4), pp. 719–729.
[71] Dembele, S., Delmas, A., and Sacadura, J.-F., 1997, "A Method for Modeling the Mitigation of Hazardous Fire Thermal Radiation by Water Spray Curtains," ASME J. Heat Transfer, **119**(4), pp. 746–753.
[72] Dembele, S., and Wen, J. X., 2000, "Investigation of a Spectral Formulation for Radiative Heat Transfer in a One-Dimensional Fires and Combustion System," Int. J. Heat Mass Transfer, **43**, pp. 4019–4030.
[73] Tang, K. C., and Brewster, M. Q., 1998, "Analysis of Molecular Gas Radiation: Real Gas Property Effects," 7th AIAA/ASME Joint Thermophysics and Heat Transfer Conference, ASME, Vol. HTD-357-1, pp. 23–32.
[74] Pierrot, L., Soufiani, A., and Taine, J., 1999, "Accuracy of Narrow-Band and Global Models for Radiative Transfer in H_2O, CO_2, and H_2O–CO_2 Mixtures at High Temperature," J. Quant. Spectrosc. Radiat. Transfer, **62**, pp. 523–548.
[75] Pierrot, L., Rivière, P., Soufiani, A., and Taine, J., 1999, "A Fictitious-Gas-Based Absorption Distribution Function Global Model for Radiative Transfer in Hot Gases," J. Quant. Spectrosc. Radiat. Transfer, **62**, pp. 609–624.
[76] Liu, F., Smallwood, G. J., and Gülder, Ö. L., 2000, "Application of the Statistical Narrow-Band Correlated-k Method to Low-Resolution Spectral Intensity and Radiative Heat Transfer Calculations—Effects of the Quadrature," Int. J. Heat Mass Transfer, **43**, pp. 3119–3135.
[77] Liu, F., and Smallwood, G. J., 2004, "An Efficient Approach for the Implementation of the SNB Based Correlated-k Method and Its Evaluation," J. Quant. Spectrosc. Radiat. Transfer, **84**, pp. 465–475.
[78] Tessé, L., Dupoirieux, F., Zamuner, B., and Taine, J., 2002, "Radiative Transfer in Real Gases Using Reciprocal and Forward Monte Carlo Methods and a Correlated-k Approach," Int. J. Heat Mass Transfer, **45**, pp. 2797–2814.

[79] Denison, M. K., and Webb, B. W., 1993, "An Absorption-Line Blackbody Distribution Function for Efficient Calculation of Total Gas Radiative Transfer," J. Quant. Spectrosc. Radiat. Transfer, **50**, pp. 499–510.
[80] Denison, M. K., and Webb, B. W., 1995, "The Spectral Line-Based Weighted-Sum-of-Gray-Gases Model in Nonisothermal Nonhomogeneous Media," ASME J. Heat Transfer, **117**(2), pp. 359–365.
[81] Modest, M. F., and Mehta, R. S., 2004, "Full Spectrum *k*-Distribution Correlations for CO_2 From the CDSD-1000 Spectroscopic Databank," Int. J. Heat Mass Transfer, **47**, pp. 2487–2491.
[82] Modest, M. F., 2003, "Narrow-Band and Full-Spectrum *k*-Distributions for Radiative Heat Transfer—Correlated-*k* vs. Scaling Approximation," J. Quant. Spectrosc. Radiat. Transfer, **76**(1), pp. 69–83.
[83] Zhang, H., and Modest, M. F., 2003, "Full-Spectrum *k*-Distribution Correlations for Carbon Dioxide Mixtures," J. Thermophys. Heat Transfer, **17**(2), pp. 259–263.
[84] Modest, M. F., and Singh, V., 2005, "Engineering Correlations for Full Spectrum *k*-Distribution of H_2O From the HITEMP Spectroscopic Databank," J. Quant. Spectrosc. Radiat. Transfer, **93**, pp. 263–271.
[85] Liu, F., Chu, H., Zhou, H., and Smallwood, G. J., 2012, "Evaluation of the Absorption Line Blackbody Distribution Function of CO_2 and H_2O Using the Proper Orthogonal Decomposition and Hyperbolic Correlations," Proceedings of Eurotherm Seminar 95, Elsevier, Nancy, France.
[86] Solovjov, V. P., and Webb, B. W., 2000, "SLW Modeling of Radiative Transfer in Multicomponent Gas Mixtures," J. Quant. Spectrosc. Radiat. Transfer, **65**, pp. 655–672.
[87] Wang, L., and Modest, M. F., 2005, "Narrow-Band Based Multiscale Full-Spectrum *k*-Distribution Method for Radiative Transfer in Inhomogeneous Gas Mixtures," ASME J. Heat Transfer, **127**(7), pp. 740–748.
[88] Pal, G., and Modest, M. F., 2009, "A Multi-Scale Full-Spectrum *k*-Distribution Method for Radiative Transfer in Nonhomogeneous Gas–Soot Mixture With Wall Emission," Comput. Thermal Sci., **1**, pp. 137–158.
[89] Zhang, H., and Modest, M. F., 2003, "Scalable Multi-Group Full-Spectrum Correlated-*k* Distributions for Radiative Heat Transfer," ASME J. Heat Transfer, **125**(3), pp. 454–461.
[90] Pal, G., and Modest, M. F., 2010, "A Narrow Band-Based Multiscale Multi-group Full-Spectrum *k*-Distribution Method for Radiative Transfer in Nonhomogeneous Gas–Soot Mixture," ASME J. Heat Transfer, **132**(2), p. 023307.
[91] Kent, J. H., and Honnery, D., 1987, "Modeling Sooting Turbulent Jet Flames Using an Extended Flamelet Technique," Combust. Sci. Technol., **54**, pp. 383–397.
[92] Mehta, R. S., Haworth, D. C., and Modest, M. F., 2010, "Composition PDF/Photon Monte Carlo Modeling of Moderately Sooting Turbulent Jet Flames," Combust. Flame, **157**, pp. 982–994.
[93] Mazumder, S., and Modest, M. F., 2002, "Application of the Full Spectrum Correlated-*k* Distribution Approach to Modeling Non-Gray Radiation in Combustion Gases," Combust. Flame, **129**(4), pp. 416–438.
[94] Sun, X., and Smith, P. J., 2010, "A Parametric Case Study in Radiative Heat Transfer Using the Reverse Monte-Carlo Ray-Tracing With Full-Spectrum *k*-Distribution Method," ASME J. Heat Transfer, **132**(2), p. 024501.
[95] Porter, R., Liu, F., Pourkashanian, M., Williams, A., and Smith, D., 2010, "Evaluation of Solution Methods for Radiative Heat Transfer in Gaseous Oxy-Fuel Combustion Environments," J. Quant. Spectrosc. Radiati. Transfer, **111**(14), pp. 2084–2094.
[96] Demarco, R., Consalvi, J. L., Fuentes, A., and Melis, S., 2011, "Assessment of Radiative Property Models in Non-Gray Sooting Media," Int. J. Thermal Sci., **50**, pp. 1672–1684.
[97] Pawlak, D. T., Clothiaux, E. E., Modest, M. F., and Cole, J. N. S., 2004, "Full Spectrum Correlated-*k* for Shortwave Atmospheric Radiative Transfer," J. Atmos. Sci., **61**, pp. 2588–2601.
[98] Hogan, R. J., 2010, "The Full-Spectrum Correlated-*k* Method for Longwave Atmospheric Radiative Transfer Using an Effective Planck Function," J. Atmos. Sci., **67**, pp. 2086–2100.
[99] Bansal, A., Modest, M. F., and Levin, D. A., 2011, "Multi-Scale *k*-Distribution Model for Gas Mixtures in Hypersonic Nonequilibrium Flows," J. Quant. Spectrosc. Radiat. Transfer, **112**(7), pp. 1213–1221.
[100] Bansal, A., and Modest, M. F., 2011, "Multiscale Part-Spectrum *k*-Distribution Database for Atomic Radiation in Hypersonic Nonequilibrium Flows," ASME J. Heat Transfer, **133**(12), p. 122701.